EUROPEAN ORGANIZATION FOR NUCLEAR RESEARCH (CERN)

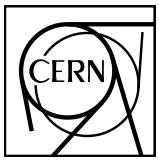

CERN-EP-2024-330
04 December 2024

Measurement of *CP* asymmetries in $\Lambda_b^0 \to ph^-$ decays

LHCb collaboration[†]

Abstract

A search for *CP* violation in $\Lambda_b^0 \to pK^-$ and $\Lambda_b^0 \to p\pi^-$ decays is presented using the full Run 1 and Run 2 data samples of pp collisions collected with the LHCb detector, corresponding to an integrated luminosity of $9\,\text{fb}^{-1}$ at center-of-mass energies of 7, 8, and 13 TeV. For the Run 2 data sample, the *CP*-violating asymmetries are measured to be $A_{CP}^{pK^-} = (-1.4 \pm 0.7 \pm 0.4)\%$ and $A_{CP}^{p\pi^-} = (0.4 \pm 0.9 \pm 0.4)\%$, where the first uncertainty is statistical and the second is systematic. Following significant improvements in the evaluation of systematic uncertainties compared to the previous LHCb measurement, the Run 1 dataset is reanalyzed to update the corresponding results. When combining the Run 2 and updated Run 1 measurements, the final results are found to be $A_{CP}^{pK^-} = (-1.1 \pm 0.7 \pm 0.4)\%$ and $A_{CP}^{p\pi^-} = (0.2 \pm 0.8 \pm 0.4)\%$, constituting the most precise measurements of these asymmetries to date.

Submitted to Phys. Rev. D

[†]Authors are listed at the end of this paper.

1 Introduction

The Standard Model (SM) of particle physics predicts the noninvariance of weak interactions under the combined application of charge conjugation (C) and parity (P) transformations via the Cabibbo–Kobayashi–Maskawa mechanism [1, 2]. In the baryon sector, many searches for CP violation (CPV) have been performed [3–19], with the only evidence coming from a recent analysis of the decay $\Lambda_b^0 \to \Lambda K^+ K^-$ [20]. In this scenario, $\Lambda_b^0 \to pK^-$ and $\Lambda_b^0 \to p\pi^-$ decays[1] are promising candidates to search for CPV, as they are mediated by the same quark-level transitions that contribute to charmless two-body $B^0 \to K^+\pi^-$ and $B_s^0 \to \pi^+ K^-$ decays, where CPV is well established [13, 21–26].

In the SM, predictions for the CP asymmetries in decays of the Λ_b^0 baryon to two-body charmless final states pK^- or $p\pi^-$ are characterized by relatively large uncertainties. These arise from difficulties in computing the hadronic parameters due to residual quantum chromodynamic (QCD) interactions between the quarks, with values of a few percent reported both in the generalized factorization approach [27, 28] and in the MIT bag model [29]. Recently, it has been suggested that the destructive interference between different partial waves in these two decays could explain the smallness of the measured CP asymmetries [30]. Measurements of these quantities were performed by the CDF and LHCb collaborations [12–14]. The world averages, dominated by the Run 1 LHCb measurement, show asymmetries compatible with zero within uncertainties of 2.2% and 2.9% for $\Lambda_b^0 \to pK^-$ and $\Lambda_b^0 \to p\pi^-$ decays, respectively [31].

This paper presents a search for CP violation in $\Lambda_b^0 \to pK^-$ and $\Lambda_b^0 \to p\pi^-$ decays, using proton-proton (pp) collision data collected with the LHCb detector at center-of-mass energies of 7, 8, and 13 TeV and corresponding to $9\,\text{fb}^{-1}$ of integrated luminosity. The dataset has been collected in two data-taking campaigns, called Run 1 (2011–2012) and Run 2 (2015–2018). The CP asymmetry is defined as

$$A_{CP}^f \equiv \frac{\Gamma(\Lambda_b^0 \to f) - \Gamma(\overline{\Lambda}_b^0 \to \overline{f})}{\Gamma(\Lambda_b^0 \to f) + \Gamma(\overline{\Lambda}_b^0 \to \overline{f})}, \tag{1}$$

where Γ is the partial width of the given decay, with $f \in \{pK^-, p\pi^-\}$ and $\overline{f} \in \{\overline{p}K^+, \overline{p}\pi^+\}$.

The rest of the paper is organized as follows. After a brief description of the detector, trigger and simulation in Sec. 2, the formalism needed to relate the physical CP asymmetries to the experimental measurements is presented in Sec. 3. The event selection and fits to the invariant-mass distributions are described in Secs. 4 and 5, respectively. The determination of instrumental asymmetries is discussed in Sec. 6, while the estimation of systematic uncertainties are presented in Sec. 7. Finally, the results are given and conclusions drawn in Sec. 8.

2 Detector, trigger and simulation

The LHCb detector [32, 33] is a single-arm forward spectrometer covering the pseudorapidity range $2 < \eta < 5$, designed for the study of particles containing b or c quarks. The detector includes a high-precision tracking system consisting of a silicon-strip vertex detector (VELO) surrounding the pp interaction region, a large-area silicon-strip detector

[1] Unless stated otherwise, the inclusion of charge-conjugate processes is implied throughout this paper.

located upstream of a dipole magnet with a bending power of about 4 T m, and three stations of silicon-strip detectors and straw drift tubes placed downstream of the magnet. The tracking system provides a measurement of the momentum, p, of charged particles with a relative uncertainty that varies from 0.5% at low momentum to 1.0% at 200 GeV/c. The minimum distance of a track to a primary vertex (PV), the impact parameter (IP), is measured with a resolution of $(15 + 29/p_{\rm T})\,\mu$m, where $p_{\rm T}$ is the component of the momentum transverse to the beam, in GeV/c. The magnetic field deflects particles in opposite directions based on their charge, which can lead to detection asymmetries. To reduce such effects, the magnet polarity is reversed periodically throughout the data taking. Different types of charged hadrons are distinguished using information from two ring-imaging Cherenkov (RICH) detectors [34]. Photons, electrons and hadrons are identified by a calorimeter system consisting of a preshower and a scintillating-pad detector (SPD), an electromagnetic and a hadronic calorimeter. Muons are identified by a system composed of alternating layers of iron and multiwire proportional chambers.

The online event selection is performed by a trigger, which consists of a hardware stage followed by a two-level software stage which applies a full event reconstruction. At the hardware trigger stage, events are required to contain a hadron with transverse energy deposited in the calorimeters greater than approximately 3.7 GeV in Run 1 and 4.0 GeV in Run 2. The first stage of the software trigger requires the presence of at least one charged particle with $p_{\rm T} > 1.6\,{\rm GeV}/c$ and consistent with originating from a displaced secondary vertex. In the second software stage, a specific algorithm is used which inclusively reconstructs decays of beauty hadrons to charged two-body final states. During Run 2, in between the two software stages, an alignment and calibration of the detector were performed in near real-time [35], ensuring the availability of high-quality tracking and particle-identification (PID) information at the trigger level.

Simulation is used to optimize the offline event selection and to develop the invariant-mass models to be applied to data. In the simulation, pp collisions are generated using Pythia [36] with a specific LHCb configuration [37]. Decays of unstable particles are described by EvtGen [38], in which final-state radiation is generated using Photos [39]. The interaction of the generated particles with the detector, and its response, are implemented using the Geant4 toolkit [40] as described in Ref. [41].

3 Analysis strategy

Two different strategies have been employed to extract the *CP* asymmetries from the Run 1 and Run 2 samples, due to the absence of a measurement of the Λ_b^0 baryon production asymmetry for the latter. For the Run 1 samples, the *CP* asymmetries of $\Lambda_b^0 \to pK^-$ and $\Lambda_b^0 \to p\pi^-$ decays are computed as the sums of various experimental quantities

$$A_{CP}^{ph^-} = A_{\rm raw}^{ph^-} - A_{\rm D}^{p} - A_{\rm D}^{h^-} - A_{\rm PID}^{ph^-} - A_{\rm T}^{ph^-} - A_{\rm P}^{\Lambda_b^0}, \tag{2}$$

where $A_{\rm raw}^{ph^-}$ is the measured raw asymmetry between the yields of the decays $\Lambda_b^0 \to ph^-$ and $\overline{\Lambda}_b^0 \to \overline{p}h^+$, with $h \in \{K, \pi\}$; $A_{\rm D}^{p}$ and $A_{\rm D}^{h^-}$ are the asymmetries between the detection efficiencies of a given hadron and its charge conjugate; $A_{\rm PID}^{ph^-}$ is the asymmetry between the PID efficiencies for the final states ph^- and $\overline{p}h^+$; $A_{\rm T}^{ph^-}$ is the asymmetry between the trigger efficiencies for the particles in the final states ph^- and $\overline{p}h^+$; and $A_{\rm P}^{\Lambda_b^0}$ is the

asymmetry between the production cross-sections of Λ_b^0 and $\overline{\Lambda}_b^0$ baryons. This linear approximation has good accuracy due to the smallness of the terms involved.

The raw asymmetry is defined as

$$A_{\rm raw}^f \equiv \frac{N(\Lambda_b^0 \to f) - N(\overline{\Lambda}_b^0 \to \overline{f})}{N(\Lambda_b^0 \to f) + N(\overline{\Lambda}_b^0 \to \overline{f})}, \tag{3}$$

where N denotes the observed signal yield for the given decay, obtained in this analysis by means of extended binned maximum-likelihood fits to the invariant-mass distributions of the 8 possible final states, namely pK^-, $\overline{p}K^+$, $p\pi^-$, $\overline{p}\pi^+$, $K^+\pi^-$, $K^-\pi^+$, K^+K^-, and $\pi^+\pi^-$, where the last four are used to constrain the yields of misidentified backgrounds in the signal channels.

The detection asymmetries are defined as

$$A_{\rm D}^{h^+} \equiv \frac{\varepsilon_{\rm rec}^{h^+} - \varepsilon_{\rm rec}^{h^-}}{\varepsilon_{\rm rec}^{h^+} + \varepsilon_{\rm rec}^{h^-}} \tag{4}$$

where $\varepsilon_{\rm rec}^{h^\pm}$, with $h \in \{p, K, \pi\}$, is the total efficiency to reconstruct the given charged particle, excluding PID and trigger requirements. Such asymmetries are mostly due to the different interaction cross-sections of particles and antiparticles with the detector material. The pion detection asymmetry has been measured from the ratio of fully to partially reconstructed $D^{*+} \to (D^0 \to K^-\pi^+\pi^+\pi^-)\pi^+$ decays [42]. The kaon detection asymmetry is obtained by first measuring the detection asymmetry of the $K^+\pi^-$ pair via the subtraction of the raw asymmetries between the $D^+ \to K_{\rm S}^0\pi^+$ and $D^+ \to K^-\pi^+\pi^+$ decay modes, and then removing the single pion detection asymmetry. The effects of CP violation and detection asymmetries for the neutral kaons are corrected according to the strategy used in Ref. [43]. The proton detection asymmetry is measured following the procedure described in Ref. [44], using as input the flight distance of protons traversing the detector in units of the nuclear interaction length. The method is validated with a combined use of a detailed LHCb detector simulation, external measurements of cross-sections of proton and antiproton scattering on deuterium targets, and information from a large calibration sample of $\Lambda \to p\pi^-$ decays. The measurement is performed with Run 2 data and used for both Run 1 and Run 2 samples. The validity of this approach is based on the assumption that the material budget of the detector did not change significantly between the two data-taking periods, as the only change to the detector was the removal of the aerogel radiator from one of the two RICH detectors.

The PID asymmetries are measured from large calibration samples of $D^{*+} \to (D^0 \to K^-\pi^+)\pi^+$ decays for pions and kaons, and $\Lambda \to p\pi^-$ and $\Lambda_c^+ \to pK^-\pi^+$ decays for protons [45]. They are defined as

$$A_{\rm PID}^{ph^-} \equiv \frac{\varepsilon_{\rm PID}^{ph^-} - \varepsilon_{\rm PID}^{\overline{p}h^+}}{\varepsilon_{\rm PID}^{ph^-} + \varepsilon_{\rm PID}^{\overline{p}h^+}}, \tag{5}$$

where $\varepsilon_{\rm PID}^f$ is the PID efficiency for a final state f given a set of PID requirements.

Asymmetries arising from different efficiencies on oppositely charged particles for the hardware and software trigger, $A_{\rm T}^{ph^-}$, may bias the results. They are defined similarly to Eq. (5), and are estimated with data-driven techniques, whose details are given in Sec. 6.

The Λ_b^0 production asymmetry is defined as

$$A_{\rm P}^{\Lambda_b^0} \equiv \frac{\sigma(\Lambda_b^0) - \sigma(\overline{\Lambda}_b^0)}{\sigma(\Lambda_b^0) + \sigma(\overline{\Lambda}_b^0)}, \tag{6}$$

where σ denotes the inclusive production cross-section in the LHCb acceptance. The Run 1 production asymmetry has been measured using semileptonic $\Lambda_b^0 \to \Lambda_c^+ \mu^- \overline{\nu}_\mu X$ decays in Ref. [44].

For the Run 2 sample, there is no available measurement of $A_{\rm P}^{\Lambda_b^0}$, therefore a different strategy to obtain the *CP* asymmetries has been devised. Employing a control sample of $\Lambda_b^0 \to (\Lambda_c^+ \to pK^-\pi^+)\pi^-$ decays, the following formulae are used:

$$A_{CP}^{pK^-} = \Delta A_{\rm raw} - \Delta A_{\rm D}^{p} - \Delta A_{\rm D}^{K^-} - \Delta A_{\rm PID} - \Delta A_{\rm P}^{\Lambda_b^0} - \Delta A_{\rm T} - A_{\rm D}^{\pi^-} - A_{\rm D}^{\pi^+} + A_{CP}^{\Lambda_c^+\pi^-}, \tag{7}$$

$$A_{CP}^{p\pi^-} = \Delta A_{\rm raw} - \Delta A_{\rm D}^{p} - \Delta A_{\rm D}^{\pi^-} - \Delta A_{\rm PID} - \Delta A_{\rm P}^{\Lambda_b^0} - \Delta A_{\rm T} - A_{\rm D}^{K^-} - A_{\rm D}^{\pi^+} + A_{CP}^{\Lambda_c^+\pi^-}, \tag{8}$$

where ΔA indicates the difference between the asymmetries determined for the signal and control modes, and $A_{\rm D}^{\pi^-}$, $A_{\rm D}^{\pi^+}$, and $A_{\rm D}^{K^-}$ are the detection asymmetries of particles from the control sample that are not accounted for in $\Delta A_{\rm D}^{h^-}$. The *CP* asymmetry in the control sample, $A_{CP}^{\Lambda_c^+\pi^-}$, is expected to be zero in the SM, within the experimental uncertainties of this analysis. The control sample is weighted to equalize the two-dimensional distribution in the $(p_{\rm T}, \eta)$ plane of the Λ_b^0 baryon with that from $\Lambda_b^0 \to ph^-$ decays, such that the $\Delta A_{\rm P}^{\Lambda_b^0}$ term is zero by construction in Eqs. (7) and (8).

Apart from this change in strategy, there is also a different method used to determine the pion detection asymmetry for Run 2. It is measured as the ratio of pion yields from $K_{\rm S}^0 \to \pi^+\pi^-$ decays reconstructed with all the tracking detectors to those reconstructed using only the track segment in the VELO [46].

4 Event selection

An optimization of the offline event selection is performed for the Run 2 sample, using the same strategy developed for the previous Run 1 analysis. To start, b-hadron candidates are reconstructed in the second stage of the software trigger, combining pairs of oppositely charged tracks with $p_{\rm T} > 1\,{\rm GeV}/c$, that are inconsistent with originating from any PV and are required to form a common vertex. The candidates must have an invariant mass, computed assigning the pion hypothesis to both final-state tracks, in the range between 4.6 and 6.4 GeV/c^2 for Run 1 and between 4.7 and 6.2 GeV/c^2 for Run 2. Finally, each b-hadron candidate is required to be consistent with originating from a PV. Fiducial requirements in the (p, η) plane are applied to both tracks in the final state, to ensure kinematic coverage of the samples used to calibrate the PID performances. The final-state particles passing the fiducial requirements have their momentum (in GeV/c) and pseudorapidity lying inside the polygon of vertices $(p,\eta) \in \{(0, 2), (25, 2), (120, 3.75), (123, 4.2), (0, 4.2)\}$.

Particle-identification criteria are used to divide the data sample into mutually exclusive subsamples corresponding to the final-state hypotheses pK^-, $\overline{p}K^+$, $p\pi^-$, $\overline{p}\pi^+$, $K^+\pi^-$, $K^-\pi^+$, K^+K^- and $\pi^+\pi^-$. The event selection also includes requirements on the output of a boosted decision tree (BDT) classifier [47], used to reject candidates formed with random combinations of oppositely charged tracks (combinatorial background). The

BDT combines the information from the following variables: the minimum and maximum transverse momentum of the b-hadron decay products; the minimum and maximum of their impact parameters; the minimum and maximum of the logarithms of their $\chi^2_{\rm IP}$ values, where $\chi^2_{\rm IP}$ is defined as the difference in the vertex-fit χ^2 of the track's associated PV reconstructed with and without the track under consideration;[2] the χ^2 of the common-vertex fit of the two tracks and the distance of closest approach between them. The BDT also exploits the following properties of the b-hadron candidate: transverse momentum, $\chi^2_{\rm IP}$, flight distance (FD), and the χ^2 of the FD, all with respect to the PV associated to the candidate. The χ^2 of the FD is a measure of how well the decay vertex of the candidate is separated from the PV. The BDT is trained using Run 2 simulated signal decays and combinatorial background candidates from Run 2 data in the high-mass sideband, defined as $m_{\pi^+\pi^-} > 5.6\,{\rm GeV}/c^2$.

Separate optimizations of the selection criteria applied to the BDT output and the PID variables are performed for $\Lambda_b^0 \to pK^-$ and $\Lambda_b^0 \to p\pi^-$ decays. These two selections will be denoted hereafter as S_{pK^-} and $S_{p\pi^-}$, respectively. For each selection, the same BDT requirement is used to select the other final-state samples, while different PID requirements are used to separate the $K^+\pi^-$, π^+K^-, $\pi^+\pi^-$, K^+K^- final states, as well as cross-feed $p\pi^-$ (pK^-) and $\overline{p}\pi^+$ ($\overline{p}K^+$) final states for S_{pK^-} ($S_{p\pi^-}$). The optimization procedure has been designed during the Run 1 analysis [14] to obtain the best sensitivity on the raw asymmetry from Eq. (3), and is based on pseudoexperiments. The optimization is performed only for the Run 2 sample, while the same BDT and PID selection from the previous analysis is kept for the Run 1 sample [14].

In less then 1% of the events, more than one candidate is present. In such cases, all candidates but one are rejected according to a reproducible pseudorandom sequence.

Finally, the dataset is split into 12 disjoint subsets based on the year of acquisition (2011, 2012, 2015, 2016, 2017, 2018) and polarity of the dipole magnet (Up, Down). This provides two useful checks: firstly, that the measured CP asymmetries are independent of the data-taking conditions and, secondly, that any possible residual left-right asymmetry has a negligible impact on the determination of A_{CP}. The CP asymmetries are measured separately in each subsample and then averaged to obtain the final result of the measurement following the method of Ref. [48].

5 Invariant-mass fit

For each final-state hypothesis, namely pK^-, $\overline{p}K^+$, $p\pi^-$, $\overline{p}\pi^+$, $K^+\pi^-$, $K^-\pi^+$, K^+K^- and $\pi^+\pi^-$, the invariant-mass distribution of selected candidates is modeled by an appropriate probability density function. These models are used to perform a simultaneous fit to the eight invariant-mass spectra and determine the yields and raw asymmetries of all two-body b-hadron signal decays contributing to the spectra. Three categories are considered for the background: combinatorial, due to random combinations of oppositely charged particles; partially reconstructed, due to multibody b-hadron decays with one or more particles not reconstructed; and cross-feed, arising from other two-body b-hadron decays where one or both final-state particles are misidentified.

The model used to describe each signal is the sum of a Gaussian function and a Johnson S_U function [49] with common mean and width. For the high-yield channels, *i.e.*

[2]The associated PV is defined as that giving the smallest $\chi^2_{\rm IP}$ value for the b-hadron candidate.

$B^0 \to K^+\pi^-$, $B_s^0 \to K^+K^-$, and $B^0 \to \pi^+\pi^-$, an additional Gaussian function with the same mean and an independent width is added to improve the quality of the fit. The shape parameters of each model are obtained from fits to simulated samples and fixed in the fit to data, with the exception of the mean and width(s).

The combinatorial background is modeled using exponential functions, with the exception of the pK^- and $\overline{p}K^+$ spectra, for which the exponential is multiplied by a function of the form $[1 + \tanh(m)]$, where m is the invariant mass of the hadron pair, to modulate the rise of the exponential at low invariant masses. This is introduced to model the threshold effect due to the requirements applied in the software trigger on the dipion mass.

The partially reconstructed background is parameterized using ARGUS functions [50] convolved with Gaussian functions with zero mean and with the same width as used for the signal model in that channel. For the three signal decays which employ a second Gaussian, the width of the component with the highest fit fraction is used for the convolution. For the pK^- and $p\pi^-$ final states, dedicated templates are built by producing large samples of $\Lambda_b^0 \to pK^-\pi^0$ and $\Lambda_b^0 \to p\pi^-\pi^0$ decays using fast simulation [51]. The impact of the BDT requirement is modeled by studying its efficiency with fully simulated $\Lambda_b^0 \to pK^-$ decays as a function of the cosine of the angle between the flight direction of the reconstructed b-hadron and the direction of its reconstructed momentum. This variable is a good proxy for the fraction of momentum removed by the undetected particle in the multibody decays. The obtained efficiency is then used to correct the samples produced with the fast simulation, where the direction of the b-hadron momentum is obtained considering only the two charged final-state particles. The produced templates are then used directly in the fit model to describe the shape of partially reconstructed backgrounds.

Finally, the cross-feed backgrounds are modeled by applying a kernel density estimation method [52] to simulated two-body b-hadron decays. The simulated samples are first weighted using PID efficiency tables as a function of particle kinematics. The cross-feed background yields are then set to the corresponding two-body b-hadron decay yields, determined by the simultaneous fit, multiplied by appropriate PID-efficiency ratios. The efficiencies for a given PID requirement are determined from calibration samples in bins of particle momentum, pseudorapidity and hit multiplicity in the SPD, as the performances of the RICH detectors depend on such variables. They are then averaged over the corresponding distributions of background-subtracted signal candidates.

After the application of the BDT and PID requirements, an extended binned maximum-likelihood fit is performed simultaneously to the eight final-state samples for each of the two selections, S_{pK^-} and $S_{p\pi^-}$. The m_{pK^-} and $m_{p\pi^-}$ invariant-mass distributions are shown in Fig. 1 after combining all 12 subsamples, with the results of the fits also shown. About 29×10^3 and 18×10^3 signal events are found in the Run 1 and Run 2 samples for $\Lambda_b^0 \to pK^-$ and $\Lambda_b^0 \to p\pi^-$, respectively.

The fits are validated by generating a large number of pseudoexperiments according to the total probability density function of the model and performing an extended binned maximum-likelihood fit to each sample. The resulting pull distributions for $A_{\rm raw}^{pK^-}$ and $A_{\rm raw}^{p\pi^-}$ are each found to be consistent with a standard normal distribution.

The raw asymmetries in the control sample of $\Lambda_b^0 \to \Lambda_c^+\pi^-$ decays used in Eqs. (7) and (8) are measured with unbinned maximum-likelihood fits to the invariant mass of the weighted sample split into the same 12 subsets as the signal channel. The signal is modeled with a Crystal Ball function [53], the combinatorial category with an exponential function,

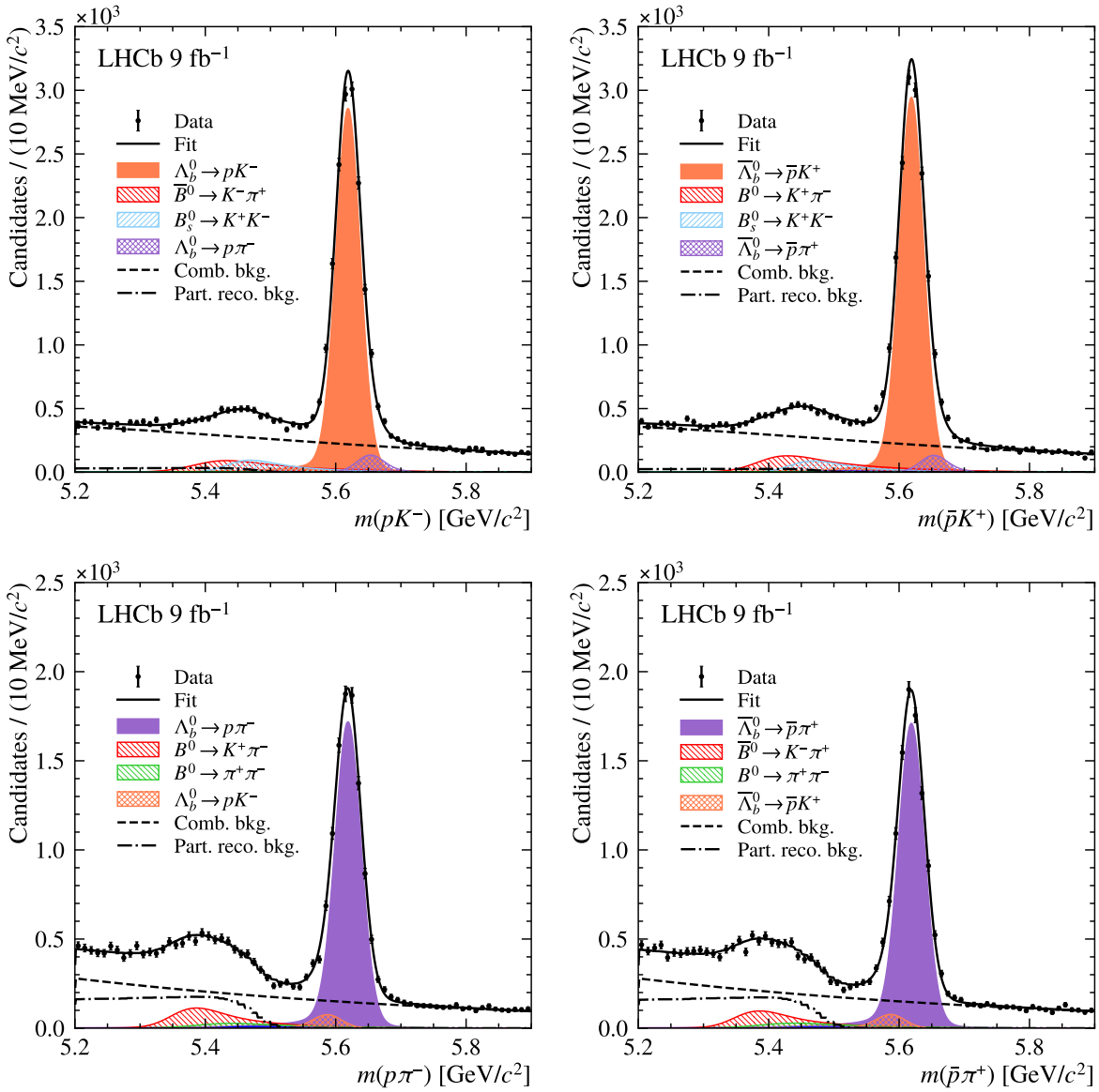

Figure 1: Invariant-mass distributions of the total Run 1 and Run 2 sample: (top left) m_{pK^-}, (top right) $m_{\overline{p}K^+}$, (bottom left) $m_{p\pi^-}$ and (bottom right) $m_{\overline{p}\pi^+}$ for candidates passing the (top) S_{pK^-} and (bottom) $S_{p\pi^-}$ selections. The results of the fits are also shown.

and the cross-feed background events from $\Lambda_b^0 \to \Lambda_c^+ K^-$ with a Gaussian distribution with the same width as the signal function and the mean shifted by the impact of the wrong mass hypothesis. About 168×10^3 signal events are found for this control sample in Run 1 and Run 2.

6 Instrumental asymmetries

Determination of the instrumental asymmetries introduced in Eqs. (2), (7), and (8) is crucial to obtain the *CP* asymmetries, as described in Sec. 3. The pion detection asymmetry is obtained by exploiting the measurements in Refs. [42] and [46] for Run 1 and Run 2,

respectively, as a function of pion momentum and pseudorapidity. The kaon detection asymmetry is determined as a function of the kaon momentum and pseudorapidity, following the approach developed in Ref. [43]. Finally, the proton detection asymmetry is measured for the Run 1 sample in Ref. [44] as a function of proton momentum. The same maps are used to obtain the Run 2 values of the proton detection asymmetries on the signal sample, given that the LHCb detector material did not change appreciably between the two data-taking campaigns. This approach is validated by the compatibility of the kaon and pion detection asymmetries between Run 1 and Run 2, at the level of 0.6 standard deviations (σ) or better. For the three types of final-state particles, a weighted average of the kinematically dependent asymmetries is evaluated over the background-subtracted [54] kinematic distributions of pions, kaons, and protons from $\Lambda_b^0 \to pK^-$, $\Lambda_b^0 \to p\pi^-$, and $\Lambda_b^0 \to \Lambda_c^+\pi^-$ decays to obtain the integrated detection asymmetries.

The PID asymmetries are computed according to Eq. (5), where the PID efficiencies for a final state f are obtained by integrating two-dimensional maps of efficiency for a set of PID requirements over the distribution of particle momentum and pseudorapidity taken from simulation. The decrease in performance with increasing event occupancy is also accounted for. The overall Λ_b^0 production asymmetry for Run 1 is calculated by averaging the production asymmetries measured as a function of Λ_b^0 rapidity [44] over the background-subtracted rapidity distributions of $\Lambda_b^0 \to pK^-$ and $\Lambda_b^0 \to p\pi^-$ candidates.

Asymmetries related to different trigger efficiencies for the charge-conjugated final states, $A_{\rm T}$, may arise. Signal candidates are classified depending on whether they are directly responsible for the affirmative decision of the trigger (denoted as a *Trigger On Signal*, or TOS candidates) or not (*Trigger Independent of Signal*, or TIS candidates). In the former case, an asymmetry can arise due to different probabilities of positively or negatively charged hadrons firing the trigger; in the latter, the same can happen to the decay products of the other b-hadron produced in the pp collision. For candidates classified as TOS at both the hardware and software stages of the LHCb trigger, the corresponding efficiency is determined using samples of $\Lambda_b^0 \to (\Lambda_c^+ \to pK^-\pi^+)\mu^-\nu X$ for protons and $B^0 \to (\overline{D}{}^0 \to K^+\pi^-)\mu^+\nu X$ decays for pions and kaons, where only the muon is required to give a positive trigger decision. For the hardware trigger, asymmetries are determined as a function of the transverse-energy deposit in the calorimeter system. For the software trigger, the $p_{\rm T}$ and $\log(\chi^2_{\rm IP})$ of the decay products are considered, as these are the variables used by the corresponding algorithms to select or reject candidates. Systematic uncertainties for this procedure are evaluated by applying the same method on simulated samples and comparing the results with the asymmetries obtained using truth information. For TIS candidates, which instead are only selected by the hardware trigger stage, the charge asymmetry is determined by studying a sample of $B^+ \to J/\psi\, K^+$ decays [55] and computing the TIS efficiency as a function of B^+ transverse momentum. The TIS asymmetry is then obtained by averaging the $p_{\rm T}$-dependent values over the background-subtracted kinematic distributions of $\Lambda_b^0 \to pK^-$ and $\Lambda_b^0 \to p\pi^-$ decays.

7 Systematic uncertainties and combination

Several sources of systematic uncertainties associated with the fit model are investigated. Alternative models are considered: the baseline model used for signal is replaced by a double-sided Crystal Ball function [53]; the templates for the cross-feed decays are

modified by excluding the correction for the PID efficiencies; the function used to model the combinatorial background is substituted with a second-order polynomial; and the templates describing the partially reconstructed backgrounds in the pK^-, $\overline{p}K^+$, $p\pi^-$, and $\overline{p}\pi^+$ spectra, defined in Sec. 5, are replaced by ARGUS functions [50]. When testing alternative models, 1000 pseudoexperiments are generated according to the baseline fit results. Fits are performed to each of the generated samples using the baseline model and then the alternative models. The mean and the root mean square of the distribution of the difference between the raw asymmetries determined by the two sets of fits are added in quadrature with the resulting value taken as a systematic uncertainty.

A different approach is adopted to assess systematic uncertainties related to the knowledge of the cross-feed background contamination. Samples are generated using the baseline fit results. The baseline model is then fitted 1000 times to the generated samples, varying the PID efficiencies according to their uncertainties, which are mainly driven by the choice of the binning scheme used to divide the phase space. On changing the binning scheme and recomputing the efficiencies, the largest deviation from the baseline is taken as a systematic uncertainty. Finally, the statistical uncertainty on the raw asymmetry extracted from the $\Lambda_b^0 \to \Lambda_c^+\pi^-$ control sample is propagated to the A_{CP} measurement, and quoted as a systematic uncertainty.

Correlations between the results in the various subsamples may arise from the use of calibration samples that are common among them, *e.g.* the use of the proton detection asymmetry measurement from Run 1 over all the Run 2 samples, or the computation of several instrumental asymmetries on the signal and control samples following Eqs. (7) and (8) with the same method. These correlations are evaluated by generating 1000 versions of the tables used to compute all the corrections, sampled from Gaussian distributions with means equal to the central values and widths equal to the nominal uncertainties. Then the 1000 sets of corrections are used to recompute $A_{CP}^{pK^-}$ and $A_{CP}^{p\pi^-}$. From the distributions of the 1000 values the correlations between the various subsamples are inferred. The correlations are found to be smaller than 8%, but are taken into account nonetheless when averaging the results.

To quantify the size of each systematic uncertainty on the final measurement, the bootstrapping procedure is repeated many times, each one varying only the baseline tables corresponding to a single correction, to decouple them from the others to which they might be correlated. This allows a breakdown of the contribution of each systematic uncertainty to the final results, which is reported in Table 1. Some systematic uncertainties are applicable to either Run 1 or Run 2 asymmetries. For instance, the use of the $\Lambda_b^0 \to \Lambda_c^+\pi^-$ control sample for Run 2 requires the evaluation of detection asymmetries for protons, kaons, and pions, as opposed to the Run 1 sample in which only two of these particles are needed for each signal channel. As this pertains to the Λ_b^0 production asymmetry, its contribution for Run 2 is removed by the kinematic weighting of the $\Lambda_b^0 \to \Lambda_c^+\pi^-$ sample, as explained in Eqs. (7) and (8). Conversely, this control sample is not needed for Run 1 as the relevant Λ_b^0 production asymmetry is measured by other means.

8 Results and conclusions

The measurements of the *CP*-violating asymmetries in the 12 individual data-taking year and magnet-polarity subsamples are found to be consistent, with a χ^2/ndf of 11.6/11 for

Table 1: Absolute systematic and statistical uncertainties, in percent, on the *CP* asymmetry measurements, split by decay channel and data-taking period. The dashes represent systematic uncertainties that do not contribute to the measurement in the corresponding sample.

	Run 1		Run 2	
	$\Lambda_b^0 \to pK^-$	$\Lambda_b^0 \to p\pi^-$	$\Lambda_b^0 \to pK^-$	$\Lambda_b^0 \to p\pi^-$
Fit model	0.1	0.2	0.1	0.2
Particle identification	0.3	0.3	0.2	0.2
TIS trigger	0.1	0.1	< 0.1	< 0.1
TOS hardware trigger	0.2	0.2	0.1	0.1
TOS software trigger	0.3	0.3	0.2	0.2
Proton detection	0.1	0.1	< 0.1	< 0.1
Kaon detection	0.3	–	0.1	< 0.1
Pion detection	–	0.1	< 0.1	< 0.1
Λ_b^0 production	0.1	0.1	–	–
$\Lambda_b^0 \to \Lambda_c^+\pi^-$ sample size	–	–	0.3	0.3
Total systematic	0.6	0.5	0.4	0.4
Statistical	1.5	1.9	0.7	0.9

$A_{CP}^{pK^-}$ and 6.7/11 for $A_{CP}^{p\pi^-}$, showing no dependence on the data-taking conditions. Using Eq. (2) in each subsample and after computing their average value according to Ref. [48], the Run 1 *CP* asymmetries are measured to be

$$A_{CP}^{pK^-} = (-0.3 \pm 1.5 \pm 0.6)\%,$$
$$A_{CP}^{p\pi^-} = (-0.6 \pm 1.9 \pm 0.5)\%,$$

where the first uncertainties are statistical and the second are systematic, with the correlation between the two measurements being 2.7%. The results are compatible with the previous result from LHCb using the same dataset [14]. While the updated measurements have larger statistical uncertainties due to the PID fiducial requirements, the systematic and total uncertainties are significantly reduced, in particular due to the new determination of the Λ_b^0 production asymmetry [44]. As an additional cross-check, the method formalized in Eqs. (7) and (8) is also used to measure the Run 1 *CP* asymmetries, obtaining compatible results. The Run 2 *CP* asymmetries, measured following Eqs. (7) and (8), are similarly averaged over the Run 2 samples to obtain

$$A_{CP}^{pK^-} = (-1.4 \pm 0.7 \pm 0.4)\%,$$
$$A_{CP}^{p\pi^-} = (\ \ 0.4 \pm 0.9 \pm 0.4)\%,$$

with a correlation of 9.8%. These values are compatible with the Run 1 results, with which they are combined to obtain the final results

$$A_{CP}^{pK^-} = (-1.1 \pm 0.7 \pm 0.4)\%,$$
$$A_{CP}^{p\pi^-} = (\ \ 0.2 \pm 0.8 \pm 0.4)\%,$$

with a total correlation of 9.6%. No evidence of *CP* violation is found. These are the most precise measurements of these observables to date, improving over the current world averages by a factor of three. These results supersede those previously obtained by LHCb [14], and will help in constraining theoretical models for QCD effects contributing to these two-body baryonic decays.

Acknowledgements

We express our gratitude to our colleagues in the CERN accelerator departments for the excellent performance of the LHC. We thank the technical and administrative staff at the LHCb institutes. We acknowledge support from CERN and from the national agencies: CAPES, CNPq, FAPERJ and FINEP (Brazil); MOST and NSFC (China); CNRS/IN2P3 (France); BMBF, DFG and MPG (Germany); INFN (Italy); NWO (Netherlands); MNiSW and NCN (Poland); MCID/IFA (Romania); MICIU and AEI (Spain); SNSF and SER (Switzerland); NASU (Ukraine); STFC (United Kingdom); DOE NP and NSF (USA). We acknowledge the computing resources that are provided by CERN, IN2P3 (France), KIT and DESY (Germany), INFN (Italy), SURF (Netherlands), PIC (Spain), GridPP (United Kingdom), CSCS (Switzerland), IFIN-HH (Romania), CBPF (Brazil), and Polish WLCG (Poland). We are indebted to the communities behind the multiple open-source software packages on which we depend. Individual groups or members have received support from ARC and ARDC (Australia); Key Research Program of Frontier Sciences of CAS, CAS PIFI, CAS CCEPP, Fundamental Research Funds for the Central Universities, and Sci. & Tech. Program of Guangzhou (China); Minciencias (Colombia); EPLANET, Marie Skłodowska-Curie Actions, ERC and NextGenerationEU (European Union); A*MIDEX, ANR, IPhU and Labex P2IO, and Région Auvergne-Rhône-Alpes (France); AvH Foundation (Germany); ICSC (Italy); Severo Ochoa and María de Maeztu Units of Excellence, GVA, XuntaGal, GENCAT, InTalent-Inditex and Prog. Atracción Talento CM (Spain); SRC (Sweden); the Leverhulme Trust, the Royal Society and UKRI (United Kingdom).

References

[1] N. Cabibbo, *Unitary symmetry and leptonic decays*, Phys. Rev. Lett. **10** (1963) 531.

[2] M. Kobayashi and T. Maskawa, *CP-violation in the renormalizable theory of weak interaction*, Prog. Theor. Phys. **49** (1973) 652.

[3] LHCb collaboration, R. Aaij *et al.*, *Searches for Λ_b^0 and Ξ_b^0 decays to $K^0_S p\pi^-$ and $K^0_S pK^-$ final states with first observation of the $\Lambda_b^0 \to K^0_S p\pi^-$ decay*, JHEP **04** (2014) 087, arXiv:1402.0770.

[4] LHCb collaboration, R. Aaij *et al.*, *Observation of the $\Lambda_b^0 \to J/\psi p\pi^-$ decay*, JHEP **07** (2014) 103, arXiv:1406.0755.

[5] LHCb collaboration, R. Aaij *et al.*, *Observation of the $\Lambda_b^0 \to \Lambda\phi$ decay*, Phys. Lett. **B759** (2016) 282, arXiv:1603.02870.

[6] LHCb collaboration, R. Aaij *et al.*, *Observations of $\Lambda_b^0 \to \Lambda K^+\pi^-$ and $\Lambda_b^0 \to \Lambda K^+K^-$ decays and searches for other Λ_b^0 and Ξ_b^0 decays to Λh^+h^- final states*, JHEP **05** (2016) 081, arXiv:1603.00413.

[7] LHCb collaboration, R. Aaij *et al.*, *Measurement of matter-antimatter differences in beauty baryon decays*, Nature Physics **13** (2017) 391, arXiv:1609.05216.

[8] LHCb collaboration, R. Aaij *et al.*, *Search for CP violation and observation of P violation in $\Lambda_b^0 \to p\pi^-\pi^+\pi^-$ decays*, Phys. Rev. **D102** (2020) 051101, arXiv:1912.10741.

[9] LHCb collaboration, R. Aaij *et al.*, *Observation of the decay $\Lambda_b^0 \to pK^-\mu^+\mu^-$ and search for CP violation*, JHEP **06** (2017) 108, arXiv:1703.00256.

[10] LHCb collaboration, R. Aaij *et al.*, *Search for CP violation in $\Lambda_c^+ \to pK^-K^+$ and $\Lambda_c^+ \to p\pi^-\pi^+$ decays*, JHEP **03** (2018) 182, arXiv:1712.07051.

[11] LHCb collaboration, R. Aaij *et al.*, *Search for CP violation using triple product asymmetries in $\Lambda_b^0 \to pK^-\pi^+\pi^-$, $\Lambda_b^0 \to pK^-K^+K^-$, and $\Xi_b^0 \to pK^-K^-\pi^+$ decays*, JHEP **08** (2018) 039, arXiv:1805.03941.

[12] CDF collaboration, T. Aaltonen *et al.*, *Measurements of direct CP violating asymmetries in charmless decays of strange bottom mesons and bottom baryons*, Phys. Rev. Lett. **106** (2011) 181802, arXiv:1103.5762.

[13] CDF collaboration, T. A. Aaltonen *et al.*, *Measurements of direct CP-violating asymmetries in charmless decays of bottom baryons*, Phys. Rev. Lett. **113** (2014) 242001, arXiv:1403.5586.

[14] LHCb collaboration, R. Aaij *et al.*, *Search for CP violation in $\Lambda_b^0 \to pK^-$ and $\Lambda_b^0 \to p\pi^-$ decays*, Phys. Lett. **B784** (2018) 101, arXiv:1807.06544.

[15] LHCb collaboration, R. Aaij *et al.*, *Measurement of CP asymmetries in charmless four-body Λ_b^0 and Ξ_b^0 decays*, Eur. Phys. J. **C79** (2019) 745, arXiv:1903.06792.

[16] LHCb collaboration, R. Aaij *et al.*, *Search for CP violation in $\Xi_c^+ \to pK^-\pi^+$ decays with model-independent techniques*, Eur. Phys. J. **C80** (2020) 986, arXiv:2006.03145.

[17] LHCb collaboration, R. Aaij *et al.*, *Search for CP violation in $\Xi_b^- \to pK^-K^-$decays*, Phys. Rev. **D104** (2021) 052010, arXiv:2104.15074.

[18] LHCb collaboration, R. Aaij *et al.*, *Observation of the suppressed $\Lambda_b^0 \to DpK^-$ decay with $D \to K^+\pi^-$ and measurement of its CP asymmetry*, Phys. Rev. **D104** (2021) 112008, arXiv:2109.02621.

[19] LHCb collaboration, R. Aaij *et al.*, *Measurement of the photon polarization in $\Lambda_b^0 \to \Lambda\gamma$ decays*, Phys. Rev. **D105** (2022) 051104, arXiv:2111.10194.

[20] LHCb collaboration, R. Aaij *et al.*, *Study of Λ_b^0 and Ξ_b^0 decays to $\Lambda h^+h'^-$ and evidence for CP violation in $\Lambda_b^0 \to \Lambda K^+K^-$*, arXiv:2411.15441, Submitted to Phys. Rev. Lett.

[21] Belle collaboration, S. W. Lin *et al.*, *Difference in direct charge-parity violation between charged and neutral B meson decays*, Nature **452** (2008) 332.

[22] LHCb collaboration, R. Aaij *et al.*, *First evidence of direct CP violation in charmless two-body decays of B_s^0 mesons*, Phys. Rev. Lett. **108** (2012) 201601, arXiv:1202.6251.

[23] Belle collaboration, Y.-T. Duh *et al.*, *Measurements of branching fractions and direct CP asymmetries for $B \to K\pi$, $B \to \pi\pi$ and $B \to KK$ decays*, Phys. Rev. **D87** (2013) 031103.

[24] BaBar collaboration, J. P. Lees *et al.*, *Measurement of CP asymmetries and branching fractions in charmless two-body B-meson decays to pions and kaons*, Phys. Rev. **D87** (2013) 052009.

[25] LHCb collaboration, R. Aaij *et al.*, *Measurement of CP asymmetries in two-body $B_{(s)}^0$-meson decays to charged pions and kaons*, Phys. Rev. **D98** (2018) 032004, arXiv:1805.06759.

[26] LHCb collaboration, R. Aaij *et al.*, *Observation of CP violation in two-body $B_{(s)}^0$-meson decays to charged pions and kaons*, JHEP **03** (2021) 075, arXiv:2012.05319.

[27] Y. K. Hsiao, Y. Yao, and C. Q. Geng, *Charmless two-body anti-triplet b-baryon decays*, Phys. Rev. **D95** (2017) 093001, arXiv:1702.05263.

[28] J. Zhu, Z.-T. Wei, and H.-W. Ke, *Semileptonic and nonleptonic weak decays of Λ_b^0*, Phys. Rev. **D99** (2019) 054020, arXiv:1803.01297.

[29] C.-Q. Geng, C.-W. Liu, and T.-H. Tsai, *Nonleptonic two-body weak decays of Λ_b in modified MIT bag model*, Phys. Rev. **D102** (2020) 034033, arXiv:2007.09897.

[30] J.-X. Yu *et al.*, *Establishing CP violation in b-baryon decays*, arXiv:2409.02821.

[31] Particle Data Group, S. Navas *et al.*, *Review of particle physics*, Phys. Rev. **D110** (2024) 030001.

[32] LHCb collaboration, A. A. Alves Jr. *et al.*, *The LHCb detector at the LHC*, JINST **3** (2008) S08005.

[33] LHCb collaboration, R. Aaij *et al.*, *LHCb detector performance*, Int. J. Mod. Phys. **A30** (2015) 1530022, arXiv:1412.6352.

[34] M. Adinolfi *et al.*, *Performance of the LHCb RICH detector at the LHC*, Eur. Phys. J. **C73** (2013) 2431, arXiv:1211.6759.

[35] G. Dujany and B. Storaci, *Real-time alignment and calibration of the LHCb Detector in Run II*, J. Phys. Conf. Ser. **664** (2015) 082010.

[36] T. Sjöstrand, S. Mrenna, and P. Skands, *A brief introduction to PYTHIA 8.1*, Comput. Phys. Commun. **178** (2008) 852, arXiv:0710.3820.

[37] I. Belyaev *et al.*, *Handling of the generation of primary events in Gauss, the LHCb simulation framework*, J. Phys. Conf. Ser. **331** (2011) 032047.

[38] D. J. Lange, *The EvtGen particle decay simulation package*, Nucl. Instrum. Meth. **A462** (2001) 152.

[39] P. Golonka and Z. Was, *PHOTOS Monte Carlo: A precision tool for QED corrections in Z and W decays*, Eur. Phys. J. **C45** (2006) 97, arXiv:hep-ph/0506026.

[40] Geant4 collaboration, J. Allison *et al.*, *Geant4 developments and applications*, IEEE Trans. Nucl. Sci. **53** (2006) 270; Geant4 collaboration, S. Agostinelli *et al.*, *Geant4: A simulation toolkit*, Nucl. Instrum. Meth. **A506** (2003) 250.

[41] M. Clemencic *et al.*, *The LHCb simulation application, Gauss: Design, evolution and experience*, J. Phys. Conf. Ser. **331** (2011) 032023.

[42] LHCb collaboration, R. Aaij *et al.*, *Measurement of the CP asymmetry in B_s^0–$\overline{B}_s^0$ mixing*, Phys. Rev. Lett. **117** (2016) 061803, arXiv:1605.09768.

[43] LHCb collaboration, R. Aaij *et al.*, *Measurement of CP asymmetry in $D^0 \to K^-K^+$ and $D^0 \to \pi^-\pi^+$ decays*, JHEP **07** (2014) 041, arXiv:1405.2797.

[44] LHCb collaboration, R. Aaij *et al.*, *Observation of a $\Lambda_b^0 - \overline{\Lambda}_b^0$ production asymmetry in proton-proton collisions at $\sqrt{s} = 7$ and 8 TeV*, JHEP **10** (2021) 060, arXiv:2107.09593.

[45] R. Aaij *et al.*, *Selection and processing of calibration samples to measure the particle identification performance of the LHCb experiment in Run 2*, Eur. Phys. J. Tech. Instr. **6** (2019) 1, arXiv:1803.00824.

[46] LHCb collaboration, R. Aaij *et al.*, *Observation of the mass difference between neutral charm-meson eigenstates*, Phys. Rev. Lett. **127** (2021) 111801, Erratum ibid. **131** (2023) 079901, arXiv:2106.03744.

[47] A. Hoecker *et al.*, *TMVA 4 — Toolkit for Multivariate Data Analysis with ROOT. Users Guide.*, arXiv:physics/0703039.

[48] M. Schmelling, *Averaging correlated data*, Phys. Scripta **51** (1995) 676.

[49] N. L. Johnson, *Systems of frequency curves generated by methods of translation*, Biometrika **36** (1949) 149.

[50] ARGUS collaboration, H. Albrecht *et al.*, *Measurement of the polarization in the decay $B \to J/\psi K^*$*, Phys. Lett. **B340** (1994) 217.

[51] G. A. Cowan, D. C. Craik, and M. D. Needham, *RapidSim: an application for the fast simulation of heavy-quark hadron decays*, Comput. Phys. Commun. **214** (2017) 239, arXiv:1612.07489.

[52] K. S. Cranmer, *Kernel estimation in high-energy physics*, Comput. Phys. Commun. **136** (2001) 198, arXiv:hep-ex/0011057.

[53] T. Skwarnicki, *A study of the radiative cascade transitions between the Upsilon-prime and Upsilon resonances*, PhD thesis, Institute of Nuclear Physics, Krakow, 1986, DESY-F31-86-02.

[54] M. Pivk and F. R. Le Diberder, *sPlot: A statistical tool to unfold data distributions*, Nucl. Instrum. Meth. **A555** (2005) 356, arXiv:physics/0402083.

[55] R. Aaij *et al.*, *Design and performance of the LHCb trigger and full real-time reconstruction in Run 2 of the LHC*, JINST **14** (2019) P04013, arXiv:1812.10790.

LHCb collaboration

R. Aaij[38], A.S.W. Abdelmotteleb[57], C. Abellan Beteta[51], F. Abudinén[57], T. Ackernley[61], A. A. Adefisoye[69], B. Adeva[47], M. Adinolfi[55], P. Adlarson[82], C. Agapopoulou[14], C.A. Aidala[83], Z. Ajaltouni[11], S. Akar[11], K. Akiba[38], P. Albicocco[28], J. Albrecht[19,f], F. Alessio[49], M. Alexander[60], Z. Aliouche[63], P. Alvarez Cartelle[56], R. Amalric[16], S. Amato[3], J.L. Amey[55], Y. Amhis[14], L. An[6], L. Anderlini[27], M. Andersson[51], A. Andreianov[44], P. Andreola[51], M. Andreotti[26], D. Andreou[69], A. Anelli[31,o,49], D. Ao[7], F. Archilli[37,u], M. Argenton[26], S. Arguedas Cuendis[9,49], A. Artamonov[44], M. Artuso[69], E. Aslanides[13], R. Ataíde Da Silva[50], M. Atzeni[65], B. Audurier[12], D. Bacher[64], I. Bachiller Perea[10], S. Bachmann[22], M. Bachmayer[50], J.J. Back[57], P. Baladron Rodriguez[47], V. Balagura[15], A. Balboni[26], W. Baldini[26], L. Balzani[19], H. Bao[7], J. Baptista de Souza Leite[61], C. Barbero Pretel[47,12], M. Barbetti[27], I. R. Barbosa[70], R.J. Barlow[63], M. Barnyakov[25], S. Barsuk[14], W. Barter[59], J. Bartz[69], J.M. Basels[17], S. Bashir[40], G. Bassi[35,r], B. Batsukh[5], P. B. Battista[14], A. Bay[50], A. Beck[65], M. Becker[19], F. Bedeschi[35], I.B. Bediaga[2], N. A. Behling[19], S. Belin[47], K. Belous[44], I. Belov[29], I. Belyaev[36], G. Benane[13], G. Bencivenni[28], E. Ben-Haim[16], A. Berezhnoy[44], R. Bernet[51], S. Bernet Andres[45], A. Bertolin[33], C. Betancourt[51], F. Betti[59], J. Bex[56], Ia. Bezshyiko[51], J. Bhom[41], M.S. Bieker[19], N.V. Biesuz[26], P. Billoir[16], A. Biolchini[38], M. Birch[62], F.C.R. Bishop[10], A. Bitadze[63], A. Bizzeti, T. Blake[57], F. Blanc[50], J.E. Blank[19], S. Blusk[69], V. Bocharnikov[44], J.A. Boelhauve[19], O. Boente Garcia[15], T. Boettcher[66], A. Bohare[59], A. Boldyrev[44], C.S. Bolognani[79], R. Bolzonella[26,l], R. B. Bonacci[1], N. Bondar[44], A. Bordelius[49], F. Borgato[33], S. Borghi[63], M. Borsato[31,o], J.T. Borsuk[41], E. Bottalico[61], S.A. Bouchiba[50], M. Bovill[64], T.J.V. Bowcock[61], A. Boyer[49], C. Bozzi[26], J. D. Brandenburg[84], A. Brea Rodriguez[50], N. Breer[19], J. Brodzicka[41], A. Brossa Gonzalo[47,†], J. Brown[61], D. Brundu[32], E. Buchanan[59], L. Buonincontri[33,p], M. Burgos Marcos[79], A.T. Burke[63], C. Burr[49], J.S. Butter[56], J. Buytaert[49], W. Byczynski[49], S. Cadeddu[32], H. Cai[74], A. C. Caillet[16], R. Calabrese[26,l], S. Calderon Ramirez[9], L. Calefice[46], S. Cali[28], M. Calvi[31,o], M. Calvo Gomez[45], P. Camargo Magalhaes[2,z], J. I. Cambon Bouzas[47], P. Campana[28], D.H. Campora Perez[79], A.F. Campoverde Quezada[7], S. Capelli[31], L. Capriotti[26], R. Caravaca-Mora[9], A. Carbone[25,j], L. Carcedo Salgado[47], R. Cardinale[29,m], A. Cardini[32], P. Carniti[31,o], L. Carus[22], A. Casais Vidal[65], R. Caspary[22], G. Casse[61], M. Cattaneo[49], G. Cavallero[26,49], V. Cavallini[26,l], S. Celani[22], S. Cesare[30,n], A.J. Chadwick[61], I. Chahrour[83], M. Charles[16], Ph. Charpentier[49], E. Chatzianagnostou[38], M. Chefdeville[10], C. Chen[13], S. Chen[5], Z. Chen[7], A. Chernov[41], S. Chernyshenko[53], X. Chiotopoulos[79], V. Chobanova[81], M. Chrzaszcz[41], A. Chubykin[44], V. Chulikov[28,36], P. Ciambrone[28], X. Cid Vidal[47], G. Ciezarek[49], P. Cifra[49], P.E.L. Clarke[59], M. Clemencic[49], H.V. Cliff[56], J. Closier[49], C. Cocha Toapaxi[22], V. Coco[49], J. Cogan[13], E. Cogneras[11], L. Cojocariu[43], S. Collaviti[50], P. Collins[49], T. Colombo[49], M. Colonna[19], A. Comerma-Montells[46], L. Congedo[24], A. Contu[32], N. Cooke[60], I. Corredoira [47], A. Correia[16], G. Corti[49], J.J. Cottee Meldrum[55], B. Couturier[49], D.C. Craik[51], M. Cruz Torres[2,g], E. Curras Rivera[50], R. Currie[59], C.L. Da Silva[68], S. Dadabaev[44], L. Dai[71], X. Dai[4], E. Dall'Occo[49], J. Dalseno[47], C. D'Ambrosio[49], J. Daniel[11], A. Danilina[44], P. d'Argent[24], G. Darze[3], A. Davidson[57], J.E. Davies[63], O. De Aguiar Francisco[63], C. De Angelis[32,k], F. De Benedetti[49], J. de Boer[38], K. De Bruyn[78], S. De Capua[63], M. De Cian[22], U. De Freitas Carneiro Da Graca[2,a],

E. De Lucia[28], J.M. De Miranda[2], L. De Paula[3], M. De Serio[24,h], P. De Simone[28], F. De Vellis[19], J.A. de Vries[79], F. Debernardis[24], D. Decamp[10], V. Dedu[13], S. Dekkers[1], L. Del Buono[16], B. Delaney[65], H.-P. Dembinski[19], J. Deng[8], V. Denysenko[51], O. Deschamps[11], F. Dettori[32,k], B. Dey[77], P. Di Nezza[28], I. Diachkov[44], S. Didenko[44], S. Ding[69], L. Dittmann[22], V. Dobishuk[53], A. D. Docheva[60], C. Dong[4,b], A.M. Donohoe[23], F. Dordei[32], A.C. dos Reis[2], A. D. Dowling[69], W. Duan[72], P. Duda[80], M.W. Dudek[41], L. Dufour[49], V. Duk[34], P. Durante[49], M. M. Duras[80], J.M. Durham[68], O. D. Durmus[77], A. Dziurda[41], A. Dzyuba[44], S. Easo[58], E. Eckstein[18], U. Egede[1], A. Egorychev[44], V. Egorychev[44], S. Eisenhardt[59], E. Ejopu[63], L. Eklund[82], M. Elashri[66], J. Ellbracht[19], S. Ely[62], A. Ene[43], J. Eschle[69], S. Esen[22], T. Evans[63], F. Fabiano[32], L.N. Falcao[2], Y. Fan[7], B. Fang[7], L. Fantini[34,q,49], M. Faria[50], K. Farmer[59], D. Fazzini[31,o], L. Felkowski[80], M. Feng[5,7], M. Feo[2], A. Fernandez Casani[48], M. Fernandez Gomez[47], A.D. Fernez[67], F. Ferrari[25,j], F. Ferreira Rodrigues[3], M. Ferrillo[51], M. Ferro-Luzzi[49], S. Filippov[44], R.A. Fini[24], M. Fiorini[26,l], M. Firlej[40], K.L. Fischer[64], D.S. Fitzgerald[83], C. Fitzpatrick[63], T. Fiutowski[40], F. Fleuret[15], M. Fontana[25], L. F. Foreman[63], R. Forty[49], D. Foulds-Holt[56], V. Franco Lima[3], M. Franco Sevilla[67], M. Frank[49], E. Franzoso[26,l], G. Frau[63], C. Frei[49], D.A. Friday[63], J. Fu[7], Q. Führing[19,f,56], Y. Fujii[1], T. Fulghesu[16], E. Gabriel[38], G. Galati[24], M.D. Galati[38], A. Gallas Torreira[47], D. Galli[25,j], S. Gambetta[59], M. Gandelman[3], P. Gandini[30], B. Ganie[63], H. Gao[7], R. Gao[64], T.Q. Gao[56], Y. Gao[8], Y. Gao[6], Y. Gao[8], L.M. Garcia Martin[50], P. Garcia Moreno[46], J. García Pardiñas[49], P. Gardner[67], K. G. Garg[8], L. Garrido[46], C. Gaspar[49], L.L. Gerken[19], E. Gersabeck[63], M. Gersabeck[20], T. Gershon[57], S. Ghizzo[29,m], Z. Ghorbanimoghaddam[55], L. Giambastiani[33,p], F. I. Giasemis[16,e], V. Gibson[56], H.K. Giemza[42], A.L. Gilman[64], M. Giovannetti[28], A. Gioventù[46], L. Girardey[63], C. Giugliano[26,l], M.A. Giza[41], E.L. Gkougkousis[62], F.C. Glaser[14,22], V.V. Gligorov[16,49], C. Göbel[70], E. Golobardes[45], D. Golubkov[44], A. Golutvin[62,49,44], S. Gomez Fernandez[46], W. Gomulka[40], F. Goncalves Abrantes[64], M. Goncerz[41], G. Gong[4,b], J. A. Gooding[19], I.V. Gorelov[44], C. Gotti[31], E. Govorkova[65], J.P. Grabowski[18], L.A. Granado Cardoso[49], E. Graugés[46], E. Graverini[50,s], L. Grazette[57], G. Graziani, A. T. Grecu[43], L.M. Greeven[38], N.A. Grieser[66], L. Grillo[60], S. Gromov[44], C. Gu[15], M. Guarise[26], L. Guerry[11], V. Guliaeva[44], P. A. Günther[22], A.-K. Guseinov[50], E. Gushchin[44], Y. Guz[6,49,44], T. Gys[49], K. Habermann[18], T. Hadavizadeh[1], C. Hadjivasiliou[67], G. Haefeli[50], C. Haen[49], G. Hallett[57], M.M. Halvorsen[49], P.M. Hamilton[67], J. Hammerich[61], Q. Han[33], X. Han[22,49], S. Hansmann-Menzemer[22], L. Hao[7], N. Harnew[64], T. H. Harris[1], M. Hartmann[14], S. Hashmi[40], J. He[7,c], F. Hemmer[49], C. Henderson[66], R.D.L. Henderson[1,57], A.M. Hennequin[49], K. Hennessy[61], L. Henry[50], J. Herd[62], P. Herrero Gascon[22], J. Heuel[17], A. Hicheur[3], G. Hijano Mendizabal[51], J. Horswill[63], R. Hou[8], Y. Hou[11], N. Howarth[61], J. Hu[72], W. Hu[6], X. Hu[4,b], W. Huang[7], W. Hulsbergen[38], R.J. Hunter[57], M. Hushchyn[44], D. Hutchcroft[61], M. Idzik[40], D. Ilin[44], P. Ilten[66], A. Inglessi[44], A. Iniukhin[44], A. Ishteev[44], K. Ivshin[44], R. Jacobsson[49], H. Jage[17], S.J. Jaimes Elles[75,49,48], S. Jakobsen[49], E. Jans[38], B.K. Jashal[48], A. Jawahery[67], V. Jevtic[19,f], E. Jiang[67], X. Jiang[5,7], Y. Jiang[7], Y. J. Jiang[6], M. John[64], A. John Rubesh Rajan[23], D. Johnson[54], C.R. Jones[56], T.P. Jones[57], S. Joshi[42], B. Jost[49], J. Juan Castella[56], N. Jurik[49], I. Juszczak[41], D. Kaminaris[50], S. Kandybei[52], M. Kane[59], Y. Kang[4,b], C. Kar[11], M. Karacson[49], D. Karpenkov[44], A. Kauniskangas[50], J.W. Kautz[66],

M.K. Kazanecki[41], F. Keizer[49], M. Kenzie[56], T. Ketel[38], B. Khanji[69], A. Kharisova[44], S. Kholodenko[35,49], G. Khreich[14], T. Kirn[17], V.S. Kirsebom[31], O. Kitouni[65], S. Klaver[39], N. Kleijne[35,r], K. Klimaszewski[42], M.R. Kmiec[42], S. Koliiev[53], L. Kolk[19], A. Konoplyannikov[44], P. Kopciewicz[49], P. Koppenburg[38], M. Korolev[44], I. Kostiuk[38], O. Kot[53], S. Kotriakhova, A. Kozachuk[44], P. Kravchenko[44], L. Kravchuk[44], M. Kreps[57], P. Krokovny[44], W. Krupa[69], W. Krzemien[42], O. Kshyvanskyi[53], S. Kubis[80], M. Kucharczyk[41], V. Kudryavtsev[44], E. Kulikova[44], A. Kupsc[82], B. K. Kutsenko[13], D. Lacarrere[49], P. Laguarta Gonzalez[46], A. Lai[32], A. Lampis[32], D. Lancierini[56], C. Landesa Gomez[47], J.J. Lane[1], R. Lane[55], G. Lanfranchi[28], C. Langenbruch[22], J. Langer[19], O. Lantwin[44], T. Latham[57], F. Lazzari[35,s,49], C. Lazzeroni[54], R. Le Gac[13], H. Lee[61], R. Lefèvre[11], A. Leflat[44], S. Legotin[44], M. Lehuraux[57], E. Lemos Cid[49], O. Leroy[13], T. Lesiak[41], E. D. Lesser[49], B. Leverington[22], A. Li[4,b], C. Li[13], H. Li[72], K. Li[8], L. Li[63], M. Li[8], P. Li[7], P.-R. Li[73], Q. Li[5,7], S. Li[8], T. Li[5,d], T. Li[72], Y. Li[8], Y. Li[5], Z. Lian[4,b], X. Liang[69], S. Libralon[48], C. Lin[7], T. Lin[58], R. Lindner[49], H. Linton[62], V. Lisovskyi[50], R. Litvinov[32,49], F. L. Liu[1], G. Liu[72], K. Liu[73], S. Liu[5,7], W. Liu[8], Y. Liu[59], Y. Liu[73], Y. L. Liu[62], G. Loachamin Ordonez[70], A. Lobo Salvia[46], A. Loi[32], T. Long[56], J.H. Lopes[3], A. Lopez Huertas[46], S. López Soliño[47], Q. Lu[15], C. Lucarelli[27], D. Lucchesi[33,p], M. Lucio Martinez[79], V. Lukashenko[38,53], Y. Luo[6], A. Lupato[33,i], E. Luppi[26,l], K. Lynch[23], X.-R. Lyu[7], G. M. Ma[4,b], S. Maccolini[19], F. Machefert[14], F. Maciuc[43], B. Mack[69], I. Mackay[64], L. M. Mackey[69], L.R. Madhan Mohan[56], M. J. Madurai[54], A. Maevskiy[44], D. Magdalinski[38], D. Maisuzenko[44], J.J. Malczewski[41], S. Malde[64], L. Malentacca[49], A. Malinin[44], T. Maltsev[44], G. Manca[32,k], G. Mancinelli[13], C. Mancuso[30], R. Manera Escalero[46], F. M. Manganella[37], D. Manuzzi[25], D. Marangotto[30,n], J.F. Marchand[10], R. Marchevski[50], U. Marconi[25], E. Mariani[16], S. Mariani[49], C. Marin Benito[46], J. Marks[22], A.M. Marshall[55], L. Martel[64], G. Martelli[34,q], G. Martellotti[36], L. Martinazzoli[49], M. Martinelli[31,o], D. Martinez Gomez[78], D. Martinez Santos[81], F. Martinez Vidal[48], A. Martorell i Granollers[45], A. Massafferri[2], R. Matev[49], A. Mathad[49], V. Matiunin[44], C. Matteuzzi[69], K.R. Mattioli[15], A. Mauri[62], E. Maurice[15], J. Mauricio[46], P. Mayencourt[50], J. Mazorra de Cos[48], M. Mazurek[42], M. McCann[62], T.H. McGrath[63], N.T. McHugh[60], A. McNab[63], R. McNulty[23], B. Meadows[66], G. Meier[19], D. Melnychuk[42], F. M. Meng[4,b], M. Merk[38,79], A. Merli[50], L. Meyer Garcia[67], D. Miao[5,7], H. Miao[7], M. Mikhasenko[76], D.A. Milanes[75,x], A. Minotti[31,o], E. Minucci[28], T. Miralles[11], B. Mitreska[19], D.S. Mitzel[19], A. Modak[58], L. Moeser[19], R.A. Mohammed[64], R.D. Moise[17], S. Mokhnenko[44], E. F. Molina Cardenas[83], T. Mombächer[49], M. Monk[57,1], S. Monteil[11], A. Morcillo Gomez[47], G. Morello[28], M.J. Morello[35,r], M.P. Morgenthaler[22], J. Moron[40], W. Morren[38], A.B. Morris[49], A.G. Morris[13], R. Mountain[69], H. Mu[4,b], Z. M. Mu[6], E. Muhammad[57], F. Muheim[59], M. Mulder[78], K. Müller[51], F. Muñoz-Rojas[9], R. Murta[62], P. Naik[61], T. Nakada[50], R. Nandakumar[58], T. Nanut[49], I. Nasteva[3], M. Needham[59], N. Neri[30,n], S. Neubert[18], N. Neufeld[49], P. Neustroev[44], J. Nicolini[19], D. Nicotra[79], E.M. Niel[49], N. Nikitin[44], Q. Niu[73], P. Nogarolli[3], P. Nogga[18], C. Normand[55], J. Novoa Fernandez[47], G. Nowak[66], C. Nunez[83], H. N. Nur[60], A. Oblakowska-Mucha[40], V. Obraztsov[44], T. Oeser[17], S. Okamura[26,l], A. Okhotnikov[44], O. Okhrimenko[53], R. Oldeman[32,k], F. Oliva[59], M. Olocco[19], C.J.G. Onderwater[79], R.H. O'Neil[49], D. Osthues[19], J.M. Otalora Goicochea[3], P. Owen[51], A. Oyanguren[48], O. Ozcelik[59], F. Paciolla[35,v], A. Padee[42], K.O. Padeken[18], B. Pagare[57], P.R. Pais[22], T. Pajero[49], A. Palano[24],

M. Palutan[28], X. Pan[4,b], G. Panshin[44], L. Paolucci[57], A. Papanestis[58,49], M. Pappagallo[24,h], L.L. Pappalardo[26,l], C. Pappenheimer[66], C. Parkes[63], D. Parmar[76], B. Passalacqua[26,l], G. Passaleva[27], D. Passaro[35,r,49], A. Pastore[24], M. Patel[62], J. Patoc[64], C. Patrignani[25,j], A. Paul[69], C.J. Pawley[79], A. Pellegrino[38], J. Peng[5,7], M. Pepe Altarelli[28], S. Perazzini[25], D. Pereima[44], H. Pereira Da Costa[68], A. Pereiro Castro[47], P. Perret[11], A. Perrevoort[78], A. Perro[49,13], M.J. Peters[66], K. Petridis[55], A. Petrolini[29,m], J. P. Pfaller[66], H. Pham[69], L. Pica[35,r], M. Piccini[34], L. Piccolo[32], B. Pietrzyk[10], G. Pietrzyk[14], R. N, Pilato[61], D. Pinci[36], F. Pisani[49], M. Pizzichemi[31,o,49], V. Placinta[43], M. Plo Casasus[47], T. Poeschl[49], F. Polci[16], M. Poli Lener[28], A. Poluektov[13], N. Polukhina[44], I. Polyakov[44], E. Polycarpo[3], S. Ponce[49], D. Popov[7], S. Poslavskii[44], K. Prasanth[59], C. Prouve[81], D. Provenzano[32,k], V. Pugatch[53], G. Punzi[35,s], S. Qasim[51], Q. Q. Qian[6], W. Qian[7], N. Qin[4,b], S. Qu[4,b], R. Quagliani[49], R.I. Rabadan Trejo[57], J.H. Rademacker[55], M. Rama[35], M. Ramírez García[83], V. Ramos De Oliveira[70], M. Ramos Pernas[57], M.S. Rangel[3], F. Ratnikov[44], G. Raven[39], M. Rebollo De Miguel[48], F. Redi[30,i], J. Reich[55], F. Reiss[20], Z. Ren[7], P.K. Resmi[64], R. Ribatti[50], G. R. Ricart[15,12], D. Riccardi[35,r], S. Ricciardi[58], K. Richardson[65], M. Richardson-Slipper[59], K. Rinnert[61], P. Robbe[14,49], G. Robertson[60], E. Rodrigues[61], A. Rodriguez Alvarez[46], E. Rodriguez Fernandez[47], J.A. Rodriguez Lopez[75], E. Rodriguez Rodriguez[49], J. Roensch[19], A. Rogachev[44], A. Rogovskiy[58], D.L. Rolf[49], P. Roloff[49], V. Romanovskiy[66], A. Romero Vidal[47], G. Romolini[26], F. Ronchetti[50], T. Rong[6], M. Rotondo[28], S. R. Roy[22], M.S. Rudolph[69], M. Ruiz Diaz[22], R.A. Ruiz Fernandez[47], J. Ruiz Vidal[82,aa], J. Ryzka[40], J. J. Saavedra-Arias[9], J.J. Saborido Silva[47], R. Sadek[15], N. Sagidova[44], D. Sahoo[77], N. Sahoo[54], B. Saitta[32,k], M. Salomoni[31,49,o], I. Sanderswood[48], R. Santacesaria[36], C. Santamarina Rios[47], M. Santimaria[28], L. Santoro [2], E. Santovetti[37], A. Saputi[26,49], D. Saranin[44], A. Sarnatskiy[78], G. Sarpis[59], M. Sarpis[63], C. Satriano[36,t], A. Satta[37], M. Saur[6], D. Savrina[44], H. Sazak[17], F. Sborzacchi[49,28], L.G. Scantlebury Smead[64], A. Scarabotto[19], S. Schael[17], S. Scherl[61], M. Schiller[60], H. Schindler[49], M. Schmelling[21], B. Schmidt[49], S. Schmitt[17], H. Schmitz[18], O. Schneider[50], A. Schopper[49], N. Schulte[19], S. Schulte[50], M.H. Schune[14], R. Schwemmer[49], G. Schwering[17], B. Sciascia[28], A. Sciuccati[49], I. Segal[76], S. Sellam[47], A. Semennikov[44], T. Senger[51], M. Senghi Soares[39], A. Sergi[29,m], N. Serra[51], L. Sestini[33], A. Seuthe[19], Y. Shang[6], D.M. Shangase[83], M. Shapkin[44], R. S. Sharma[69], I. Shchemerov[44], L. Shchutska[50], T. Shears[61], L. Shekhtman[44], Z. Shen[6], S. Sheng[5,7], V. Shevchenko[44], B. Shi[7], Q. Shi[7], Y. Shimizu[14], E. Shmanin[25], R. Shorkin[44], J.D. Shupperd[69], R. Silva Coutinho[69], G. Simi[33,p], S. Simone[24,h], N. Skidmore[57], T. Skwarnicki[69], M.W. Slater[54], J.C. Smallwood[64], E. Smith[65], K. Smith[68], M. Smith[62], A. Snoch[38], L. Soares Lavra[59], M.D. Sokoloff[66], F.J.P. Soler[60], A. Solomin[44,55], A. Solovev[44], I. Solovyev[44], N. S. Sommerfeld[18], R. Song[1], Y. Song[50], Y. Song[4,b], Y. S. Song[6], F.L. Souza De Almeida[69], B. Souza De Paula[3], E. Spadaro Norella[29,m], E. Spedicato[25], J.G. Speer[19], E. Spiridenkov[44], P. Spradlin[60], V. Sriskaran[49], F. Stagni[49], M. Stahl[76], S. Stahl[49], S. Stanislaus[64], M. Stefaniak[84], E.N. Stein[49], O. Steinkamp[51], O. Stenyakin[44], H. Stevens[19], D. Strekalina[44], Y. Su[7], F. Suljik[64], J. Sun[32], L. Sun[74], D. Sundfeld[2], W. Sutcliffe[51], P.N. Swallow[54], K. Swientek[40], F. Swystun[56], A. Szabelski[42], T. Szumlak[40], Y. Tan[4,b], Y. Tang[74], M.D. Tat[22], A. Terentev[44], F. Terzuoli[35,v,49], F. Teubert[49], E. Thomas[49], D.J.D. Thompson[54], H. Tilquin[62],

V. Tisserand[11], S. T'Jampens[10], M. Tobin[5,49], L. Tomassetti[26,l], G. Tonani[30,n], X. Tong[6], T. Tork[30], D. Torres Machado[2], L. Toscano[19], D.Y. Tou[4,b], C. Trippl[45], G. Tuci[22], N. Tuning[38], L.H. Uecker[22], A. Ukleja[40], D.J. Unverzagt[22], B. Urbach[59], A. Usachov[39], A. Ustyuzhanin[44], U. Uwer[22], V. Vagnoni[25], V. Valcarce Cadenas[47], G. Valenti[25], N. Valls Canudas[49], J. van Eldik[49], H. Van Hecke[68], E. van Herwijnen[62], C.B. Van Hulse[47,y], R. Van Laak[50], M. van Veghel[38], G. Vasquez[51], R. Vazquez Gomez[46], P. Vazquez Regueiro[47], C. Vázquez Sierra[47], S. Vecchi[26], J.J. Velthuis[55], M. Veltri[27,w], A. Venkateswaran[50], M. Verdoglia[32], M. Vesterinen[57], D. Vico Benet[64], P. Vidrier Villalba[46], M. Vieites Diaz[47], X. Vilasis-Cardona[45], E. Vilella Figueras[61], A. Villa[25], P. Vincent[16], F.C. Volle[54], D. vom Bruch[13], N. Voropaev[44], K. Vos[79], C. Vrahas[59], J. Wagner[19], J. Walsh[35], E.J. Walton[1,57], G. Wan[6], C. Wang[22], G. Wang[8], H. Wang[73], J. Wang[6], J. Wang[5], J. Wang[4,b], J. Wang[74], M. Wang[49], N. W. Wang[7], R. Wang[55], X. Wang[8], X. Wang[72], X. W. Wang[62], Y. Wang[6], Y. W. Wang[73], Z. Wang[14], Z. Wang[4,b], Z. Wang[30], J.A. Ward[57,1], M. Waterlaat[49], N.K. Watson[54], D. Websdale[62], Y. Wei[6], J. Wendel[81], B.D.C. Westhenry[55], C. White[56], M. Whitehead[60], E. Whiter[54], A.R. Wiederhold[63], D. Wiedner[19], G. Wilkinson[64], M.K. Wilkinson[66], M. Williams[65], M. J. Williams[49], M.R.J. Williams[59], R. Williams[56], Z. Williams[55], F.F. Wilson[58], M. Winn[12], W. Wislicki[42], M. Witek[41], L. Witola[22], G. Wormser[14], S.A. Wotton[56], H. Wu[69], J. Wu[8], X. Wu[74], Y. Wu[6], Z. Wu[7], K. Wyllie[49], S. Xian[72], Z. Xiang[5], Y. Xie[8], T. X. Xing[30], A. Xu[35], L. Xu[4,b], L. Xu[4,b], M. Xu[57], Z. Xu[49], Z. Xu[7], Z. Xu[5], K. Yang[62], S. Yang[7], X. Yang[6], Y. Yang[29,m], Z. Yang[6], V. Yeroshenko[14], H. Yeung[63], H. Yin[8], X. Yin[7], C. Y. Yu[6], J. Yu[71], X. Yuan[5], Y Yuan[5,7], E. Zaffaroni[50], M. Zavertyaev[21], M. Zdybal[41], F. Zenesini[25], C. Zeng[5,7], M. Zeng[4,b], C. Zhang[6], D. Zhang[8], J. Zhang[7], L. Zhang[4,b], S. Zhang[71], S. Zhang[64], Y. Zhang[6], Y. Z. Zhang[4,b], Z. Zhang[4,b], Y. Zhao[22], A. Zhelezov[22], S. Z. Zheng[6], X. Z. Zheng[4,b], Y. Zheng[7], T. Zhou[6], X. Zhou[8], Y. Zhou[7], V. Zhovkovska[57], L. Z. Zhu[7], X. Zhu[4,b], X. Zhu[8], V. Zhukov[17], J. Zhuo[48], Q. Zou[5,7], D. Zuliani[33,p], G. Zunica[50].

[1] *School of Physics and Astronomy, Monash University, Melbourne, Australia*
[2] *Centro Brasileiro de Pesquisas Físicas (CBPF), Rio de Janeiro, Brazil*
[3] *Universidade Federal do Rio de Janeiro (UFRJ), Rio de Janeiro, Brazil*
[4] *Department of Engineering Physics, Tsinghua University, Beijing, China*
[5] *Institute Of High Energy Physics (IHEP), Beijing, China*
[6] *School of Physics State Key Laboratory of Nuclear Physics and Technology, Peking University, Beijing, China*
[7] *University of Chinese Academy of Sciences, Beijing, China*
[8] *Institute of Particle Physics, Central China Normal University, Wuhan, Hubei, China*
[9] *Consejo Nacional de Rectores (CONARE), San Jose, Costa Rica*
[10] *Université Savoie Mont Blanc, CNRS, IN2P3-LAPP, Annecy, France*
[11] *Université Clermont Auvergne, CNRS/IN2P3, LPC, Clermont-Ferrand, France*
[12] *Université Paris-Saclay, Centre d'Etudes de Saclay (CEA), IRFU, Saclay, France, Gif-Sur-Yvette, France*
[13] *Aix Marseille Univ, CNRS/IN2P3, CPPM, Marseille, France*
[14] *Université Paris-Saclay, CNRS/IN2P3, IJCLab, Orsay, France*
[15] *Laboratoire Leprince-Ringuet, CNRS/IN2P3, Ecole Polytechnique, Institut Polytechnique de Paris, Palaiseau, France*
[16] *LPNHE, Sorbonne Université, Paris Diderot Sorbonne Paris Cité, CNRS/IN2P3, Paris, France*
[17] *I. Physikalisches Institut, RWTH Aachen University, Aachen, Germany*
[18] *Universität Bonn - Helmholtz-Institut für Strahlen und Kernphysik, Bonn, Germany*
[19] *Fakultät Physik, Technische Universität Dortmund, Dortmund, Germany*

[20] *Physikalisches Institut, Albert-Ludwigs-Universität Freiburg, Freiburg, Germany*
[21] *Max-Planck-Institut für Kernphysik (MPIK), Heidelberg, Germany*
[22] *Physikalisches Institut, Ruprecht-Karls-Universität Heidelberg, Heidelberg, Germany*
[23] *School of Physics, University College Dublin, Dublin, Ireland*
[24] *INFN Sezione di Bari, Bari, Italy*
[25] *INFN Sezione di Bologna, Bologna, Italy*
[26] *INFN Sezione di Ferrara, Ferrara, Italy*
[27] *INFN Sezione di Firenze, Firenze, Italy*
[28] *INFN Laboratori Nazionali di Frascati, Frascati, Italy*
[29] *INFN Sezione di Genova, Genova, Italy*
[30] *INFN Sezione di Milano, Milano, Italy*
[31] *INFN Sezione di Milano-Bicocca, Milano, Italy*
[32] *INFN Sezione di Cagliari, Monserrato, Italy*
[33] *INFN Sezione di Padova, Padova, Italy*
[34] *INFN Sezione di Perugia, Perugia, Italy*
[35] *INFN Sezione di Pisa, Pisa, Italy*
[36] *INFN Sezione di Roma La Sapienza, Roma, Italy*
[37] *INFN Sezione di Roma Tor Vergata, Roma, Italy*
[38] *Nikhef National Institute for Subatomic Physics, Amsterdam, Netherlands*
[39] *Nikhef National Institute for Subatomic Physics and VU University Amsterdam, Amsterdam, Netherlands*
[40] *AGH - University of Krakow, Faculty of Physics and Applied Computer Science, Kraków, Poland*
[41] *Henryk Niewodniczanski Institute of Nuclear Physics Polish Academy of Sciences, Kraków, Poland*
[42] *National Center for Nuclear Research (NCBJ), Warsaw, Poland*
[43] *Horia Hulubei National Institute of Physics and Nuclear Engineering, Bucharest-Magurele, Romania*
[44] *Affiliated with an institute covered by a cooperation agreement with CERN*
[45] *DS4DS, La Salle, Universitat Ramon Llull, Barcelona, Spain*
[46] *ICCUB, Universitat de Barcelona, Barcelona, Spain*
[47] *Instituto Galego de Física de Altas Enerxías (IGFAE), Universidade de Santiago de Compostela, Santiago de Compostela, Spain*
[48] *Instituto de Fisica Corpuscular, Centro Mixto Universidad de Valencia - CSIC, Valencia, Spain*
[49] *European Organization for Nuclear Research (CERN), Geneva, Switzerland*
[50] *Institute of Physics, Ecole Polytechnique Fédérale de Lausanne (EPFL), Lausanne, Switzerland*
[51] *Physik-Institut, Universität Zürich, Zürich, Switzerland*
[52] *NSC Kharkiv Institute of Physics and Technology (NSC KIPT), Kharkiv, Ukraine*
[53] *Institute for Nuclear Research of the National Academy of Sciences (KINR), Kyiv, Ukraine*
[54] *School of Physics and Astronomy, University of Birmingham, Birmingham, United Kingdom*
[55] *H.H. Wills Physics Laboratory, University of Bristol, Bristol, United Kingdom*
[56] *Cavendish Laboratory, University of Cambridge, Cambridge, United Kingdom*
[57] *Department of Physics, University of Warwick, Coventry, United Kingdom*
[58] *STFC Rutherford Appleton Laboratory, Didcot, United Kingdom*
[59] *School of Physics and Astronomy, University of Edinburgh, Edinburgh, United Kingdom*
[60] *School of Physics and Astronomy, University of Glasgow, Glasgow, United Kingdom*
[61] *Oliver Lodge Laboratory, University of Liverpool, Liverpool, United Kingdom*
[62] *Imperial College London, London, United Kingdom*
[63] *Department of Physics and Astronomy, University of Manchester, Manchester, United Kingdom*
[64] *Department of Physics, University of Oxford, Oxford, United Kingdom*
[65] *Massachusetts Institute of Technology, Cambridge, MA, United States*
[66] *University of Cincinnati, Cincinnati, OH, United States*
[67] *University of Maryland, College Park, MD, United States*
[68] *Los Alamos National Laboratory (LANL), Los Alamos, NM, United States*
[69] *Syracuse University, Syracuse, NY, United States*
[70] *Pontifícia Universidade Católica do Rio de Janeiro (PUC-Rio), Rio de Janeiro, Brazil, associated to* [3]
[71] *School of Physics and Electronics, Hunan University, Changsha City, China, associated to* [8]
[72] *Guangdong Provincial Key Laboratory of Nuclear Science, Guangdong-Hong Kong Joint Laboratory of Quantum Matter, Institute of Quantum Matter, South China Normal University, Guangzhou, China,*

associated to [4]
[73] *Lanzhou University, Lanzhou, China, associated to* [5]
[74] *School of Physics and Technology, Wuhan University, Wuhan, China, associated to* [4]
[75] *Departamento de Fisica , Universidad Nacional de Colombia, Bogota, Colombia, associated to* [16]
[76] *Ruhr Universitaet Bochum, Fakultaet f. Physik und Astronomie, Bochum, Germany, associated to* [19]
[77] *Eotvos Lorand University, Budapest, Hungary, associated to* [49]
[78] *Van Swinderen Institute, University of Groningen, Groningen, Netherlands, associated to* [38]
[79] *Universiteit Maastricht, Maastricht, Netherlands, associated to* [38]
[80] *Tadeusz Kosciuszko Cracow University of Technology, Cracow, Poland, associated to* [41]
[81] *Universidade da Coruña, A Coruña, Spain, associated to* [45]
[82] *Department of Physics and Astronomy, Uppsala University, Uppsala, Sweden, associated to* [60]
[83] *University of Michigan, Ann Arbor, MI, United States, associated to* [69]
[84] *Ohio State University, Columbus, United States, associated to* [68]

[a] *Centro Federal de Educacão Tecnológica Celso Suckow da Fonseca, Rio De Janeiro, Brazil*
[b] *Center for High Energy Physics, Tsinghua University, Beijing, China*
[c] *Hangzhou Institute for Advanced Study, UCAS, Hangzhou, China*
[d] *School of Physics and Electronics, Henan University , Kaifeng, China*
[e] *LIP6, Sorbonne Université, Paris, France*
[f] *Lamarr Institute for Machine Learning and Artificial Intelligence, Dortmund, Germany*
[g] *Universidad Nacional Autónoma de Honduras, Tegucigalpa, Honduras*
[h] *Università di Bari, Bari, Italy*
[i] *Università di Bergamo, Bergamo, Italy*
[j] *Università di Bologna, Bologna, Italy*
[k] *Università di Cagliari, Cagliari, Italy*
[l] *Università di Ferrara, Ferrara, Italy*
[m] *Università di Genova, Genova, Italy*
[n] *Università degli Studi di Milano, Milano, Italy*
[o] *Università degli Studi di Milano-Bicocca, Milano, Italy*
[p] *Università di Padova, Padova, Italy*
[q] *Università di Perugia, Perugia, Italy*
[r] *Scuola Normale Superiore, Pisa, Italy*
[s] *Università di Pisa, Pisa, Italy*
[t] *Università della Basilicata, Potenza, Italy*
[u] *Università di Roma Tor Vergata, Roma, Italy*
[v] *Università di Siena, Siena, Italy*
[w] *Università di Urbino, Urbino, Italy*
[x] *Universidad de Ingeniería y Tecnología (UTEC), Lima, Peru*
[y] *Universidad de Alcalá, Alcalá de Henares , Spain*
[z] *Facultad de Ciencias Fisicas, Madrid, Spain*
[aa] *Department of Physics/Division of Particle Physics, Lund, Sweden*

[†] *Deceased*